RSC Advances

PAPER

View Article Online
View Journal | View Issue

Cite this: *RSC Adv.*, 2021, **11**, 12381

Anti-greasy and conductive superamphiphobic coating applied to the carbon brushes/conductive rings of hydro-generators

Yang Fu, [ac] Hongling Qin [*a] and Zhiguang Guo [*bc]

A superamphiphobic coating is usually prepared *via* a reduction reaction and then deposited onto the surface of the substrate. This technology is difficult to control and achieve high bond strength, which easily leads to powder shedding. To overcome this issue, electroplating technology is usually preferred for preparing adhesion coatings. However, the coating prepared using this method is usually suitable only for hard steel substrates, and not for soft substrates such as carbon brushes. Herein, we demonstrate an air spray technology for preparing anti-greasy and conductive superamphiphobic graphite-1*H*,1*H*,2*H*,2*H*-perfluorooctyltrichlorosilane–SiO_2 (GPS) coatings suitable for both soft substrates (carbon brushes) and hard substrates (collector rings). The sheet resistance of the coating with 10% graphite content is 4.8×10^{-3} Ω □$^{-1}$ for a 10 μm thin coating, corresponding to a resistivity of 4.8 μΩ cm. More importantly, the prepared coating has excellent liquid repellency, such as water, rapeseed oil and *n*-hexane. In addition, the coating has excellent anti-greasy and mechanical properties, which provide a brand-new solution for the greasy pollution in the engineering field. These advantages will enhance the application of superamphiphobic GPS coating in the fields of hydropower, wind power and transportation, and so on.

Received 2nd March 2021
Accepted 15th March 2021

DOI: 10.1039/d1ra01656c

rsc.li/rsc-advances

1. Introduction

Carbon brushes, as an important part of hydroelectric power generation systems, are usually used to transmit current and energy in hydroelectric power plants.[1–5] However, there are various problems in the excitation system of hydro-generator, such as carbon brush sparking, severe wear of the collector ring, and greasy pollution of the side of the carbon brush and collector ring. In order to avoid the severe sparking phenomenon of the carbon brush, a larger spring pressure is required, but in order to avoid a severe mechanical wear of the carbon brush, a smaller spring pressure is required.[6] These problems may reduce the ability of the carbon brushes to transfer current and even cause the failure of hydro-generators.[7–12] Therefore, from the perspective of anti-grease and self-cleaning of the carbon brush and collector ring, it is necessary to endow the carbon brush and collector ring with outstanding superamphiphobic performance. In terms of superamphiphobicity, Wu *et al.*[13] prepared SiO_2 *via* a reduction reaction and modified it to prepare a superamphiphobic coating that can be used for crude oil transportation. Zhou[14] prepared the superamphiphobic fabric with self-healing ability, which can recover its liquid repellency after being damaged by a simple heat treatment. At the same time, this superamphiphobic coating has the possibility of being used in protective clothing. Deng *et al.*[15] calcined the porous precipitates of a candle soot to prepare an impact-resistant superamphiphobic coating, which has good transparency.

Thus far, a good deal of superhydrophobic coating designs are inspired by the excellent hydrophobicity of the surfaces of some animals and plants in nature, such as lotus leaves,[16,17] butterfly and dragonfly wings[18,19] and water strider.[20–22] Superhydrophobicity is mainly related to the two major factors of surface roughness and low surface energy.[14,23–26] Because of its controllability and simple preparation, the superhydrophobic coating was diffusely used for separating oil from water, anti-icing of insulators, self-cleaning and anti-corrosion of solar panels.[27–33] However, no superoleophobic surfaces of animals or plants have been found in nature. It is said that researchers have used various techniques to produce superamphiphobic coatings that are both superoleophobic and superhydrophobic. In the preparation of the superamphiphobic coating, He *et al.*[34] used polydimethylsiloxane and SiO_2 nanoparticles to prepare superhydrophobic and nearly superoleophobic superamphiphobic coatings and then modified the coatings with

[a]*Hubei Key Laboratory of Hydroelectric Machinery Design & Maintenance, China Three Gorges University, Hubei, Yichang 443002, People's Republic of China. E-mail: qhl1120@qq.com*

[b]*Ministry of Education Key Laboratory for the Green Preparation and Application of Functional Materials, Hubei University, Wuhan 430062, People's Republic of China*

[c]*State Key Laboratory of Solid Lubrication, Lanzhou Institute of Chemical Physics, Chinese Academy of Sciences, Lanzhou 730000, People's Republic of China. E-mail: zguo@licp.cas.cn*

modifiers to show certain transparency (Table 1). This coating has the possibility of being applied to outdoor glass and other scenes. However, because of the poor mechanical properties, wear resistance and electrical conductivity of carbon brush materials, the application of carbon brush superamphiphobic coating has been limited. Considering the simplicity of the preparation of the superamphiphobic coating and the wide range of applications, carbon brushes in hydropower systems imminently need a superamphiphobic coating with superior electrical conductivity and anti-greasy performance. The design of a conductive superamphiphobic coating that has a certain degree of wear resistance and excellent electrical conductivity and that can be successfully used in a carbon brush/collector ring system is still a challenge for us.

Herein, we report an anti-greasy and conductive superamphiphobic coating that can be used in the carbon brush and collector ring of hydroelectric generators. At first, SiO_2 powder was prepared by reducing hydrazine hydrate (N_2H_4 H_2O) and modified with 1*H*,1*H*,2*H*,2*H*-perfluorooctyltrichlorosilane (PFTS). Then, a certain proportion of graphite particles were added to the above powder and evenly stirred to form superamphiphobic graphite–PFTS–SiO_2 (GPS) particles. Aluminum phosphate and modified GPS were added to ethanol and water solution, added to the spray gun and sprayed on the carbon brush and collector ring surface. The coated carbon brush surface has excellent repellency to many liquids (such as water, rapeseed oil, and hexadecane). The contact angles (CAs) of the three liquids are between 120° and 150°, and the sliding angles (SAs) are not more than 9°. The coating carbon brush also demonstrated excellent self-cleaning ability, mechanical and electrical conductivity, and anti-greasy property. At the same time, due to its anti-oil adhesion, superamphiphobic GPS coating can effectively avoid the oil-rich phenomenon on the carbon brush and collector ring. The excellent performance of the GPS coating will show great potential in the carbon brush/collector ring system, railway pantograph system, transportation and so on.

Table 1 The research history of superamphiphobic coatings based on silica

Year	Author	Main research	Ref.
2011	He	The superamphiphobic coating was prepared using polydimethylsiloxane (PDMS) and SiO_2 nanoparticles, and then sintered and treated with 1*H*,1*H*,2*H*,2*H*-perfluorooctyl-trichlorosilane (PFTS) to show transparency	34
2012	Deng	A layer of oil-rebounding, wear-resistant and transparent superamphiphobic coating is prepared by covering the silicon shell on candle soot	15
2013	Zhou	Using fluoroalkyl silane and modified SiO_2 nanoparticles through chemical coating technology, a superamphiphobic fabric that can be used in protective clothing is prepared	14
2016	Chen	The flower-like superamphiphobic FOTS-TiO_2 powder with the lowest surface tension among the powder samples was synthesized by hot solvothermal and self-assembly functionalization	16
2018	Wu	The superamphiphobic FOTS–SiO_2 coating that can be used for crude oil transportation is prepared by reduction reaction and functionalized self-assembly	13

2. Experimental section

2.1. Materials

The graphite particles were obtained by grinding the carbon brush provided by Gezhouba Group (Yichang) with an 800 mesh sandpaper. Ethyl orthosilicate (TEOS) (AR 98%) was purchased from Xilong Science Co., Ltd. Hydrazine hydrate (N_2H_4 H_2O) (AR97%) was provided by Shanghai Zhongqin Chemical Reagent Co., Ltd. 1*H*,1*H*,2*H*,2*H*-Perfluorooctyltrichlorosilane (PFTS) (AR97%) was acquired from Meryer (Shanghai) Chemical Technology Co., Ltd. Polyvinylidene fluoride-*co*-hexafluoropropylene (PVDF-HFP) (average M_w ~400 000, average M_n ~130 000, pellets) was bought from Shanghai Macklin Biochemical Co., Ltd. *N*,*N*-Dimethylformamide (AR 99.5%) and ethanol were obtained from Li'an Long Bohua (Tianjin) Pharmaceutical Chemical Co., Ltd. Sudan IV (AR 99%) was provided by Tianjin Tianxin Fine Chemical Development Center. Methylene blue (AR 82%) was provided by Aladdin Industrial Corporation. Rapeseed oil was purchased from Dachang International (Shanghai) Co., Ltd. In addition, all other chemicals were analytically pure and were used as received.

2.2. Production of superamphiphobic GPS coating

As shown in Fig. 1b, SiO_2 particles were prepared and purified *via* a typical N_2H_4 reduction reaction. During the synthesis, 15 mL TEOS was mixed with 180 mL ethanol and stirred for 10 minutes to form a clean and uniform mixture solution. Then, after stirring for 8 h using a magnetic stirrer at room temperature, 9 mL of $N_2H_4 \cdot H_2O$ was added to the above mixed solution. After the reaction, the supernatant in the beaker was poured out, and the white turbid liquid at the bottom was washed with ethanol and put into the centrifuge tube. The centrifuge tube was put into the centrifuge and washed 3 times, each time for 5 minutes. The sediment in the washed centrifuge tube was set in a 60 °C drying oven for 4 h to obtain SiO_2 nanoparticles.

Then, 1 g of prepared SiO_2 nanoparticles were dispersed in 50 mL of 0.5% 1*H*,1*H*,2*H*,2*H*-perfluorooctyltrichlorosilane (PFTS) and *n*-hexane and stirred using a magnetic stirrer for 2 h. Let the above solution stand for 2 h, and then pour out the supernatant, wash the lower sediment with ethanol solution and pour it into a centrifuge tube. The centrifuge tube was placed in a centrifuge for centrifugation and washing for 5 min, and then washed 3 times. The centrifuge tube was dried in an oven at 60 °C and dried

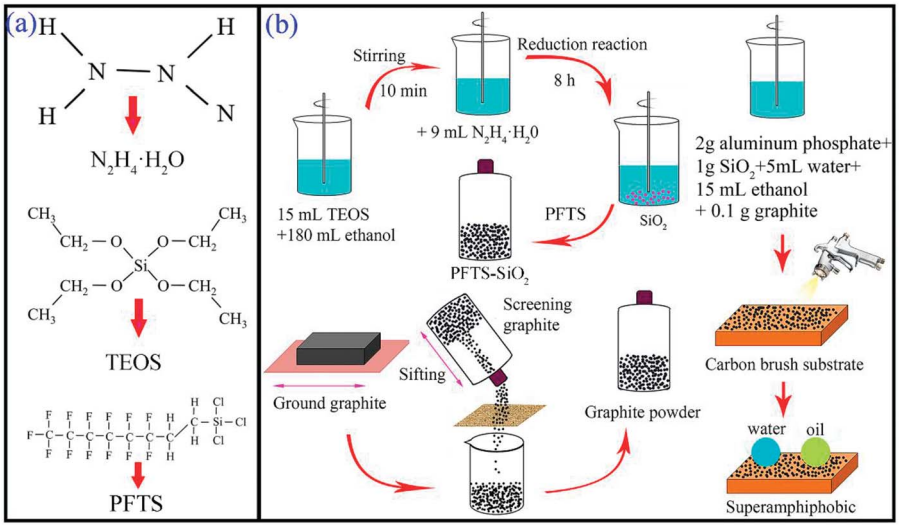

Fig. 1 (a) Structural formulas of reactants and modifiers. (b) Production of the superamphiphobic graphite–PFTS–SiO_2 powder and coating production.

for 4 h to obtain a superamphiphobic PFTS–SiO_2 powder. Finally, 2 g of aluminum phosphate solution and 5 mL of water were taken out and poured into a 50 mL beaker and placed in a shaker. 1 g of superamphiphobic PFTS–SiO_2 powder and 0.1 g of graphite powder were taken out and poured into the above solution. The above solution was shaken for 10 minutes and stirred using a magnetic stirrer for 30 minutes. Then, pour the prepared solution into the spray gun and spray it on the carbon brush, glass plate, copper plate and stainless steel substrate.

2.3. Characterization

In order to observe the microscopic morphology and chemical elements of the superamphiphobic GPS coating, the surface morphology of the carbon brush coated with superamphiphobic GPS was observed using a field emission scanning electron microscope (FEI, QUANTA FEG650). The crystal structure of the prepared GPS nanoparticles was characterized by X-ray diffraction (XRD) using an X'PERT PRO diffractometer, in which Cu Kα radiation has a wavelength of 1.5418 Å, a step size of 0.02° and a range of 2θ from 5° to 80°. The thermal stability of the coating was analyzed by Fourier transform infrared spectroscopy (FTIR, Thermo Scientific Nicolet iS10) on the GPS coating using an FTIR spectrometer. The chemical elements and functional groups of the GPS coating are analyzed by X-ray photoelectron spectroscopy (XPS) (ESCALAB 250Xi). The contact angle on the carbon brush coated with superamphiphobic GPS was measured using a contact angle meter (JC2000D). The contact angle of the same sample is averaged from 5 measurements at different locations. All optical photos were taken using a 48-megapixel mobile phone.

3. Results and discussion

3.1. Production of superamphiphobic GPS particles

Superamphiphobic graphite–PFTS–SiO_2 (GPS) particles were prepared by the reduction reaction of ethyl orthosilicate and hydrazine hydrate in ethanol and modifying 1*H*,1*H*,2*H*,2*H*-perfluorooctyltrichlorosilane (see Fig. 1). Here, SiO_2 particles with micro-nano structure were obtained *via* the reduction reaction of $N_2H_4 \cdot H_2O$ and ethyl orthosilicate in ethanol for 8 h (see Fig. 6h and i). By observing the SEM images of PFTS–SiO_2 coating with or without graphite in Fig. 2a and b, it was found that the surface microscopic morphology of the superamphiphobic coating with or without graphite is similar. However, there are significant scale-like substances on the surface of the coating after adding graphite powder, which indicates the existence of graphite scales. At the same time, the prepared GPS coating has excellent superamphiphobicity. As shown in Fig. 2c, the PFTS–SiO_2 coating with graphite powder has more P, Si and Al elements, and the rest has a small amount of C and O elements. As shown in Fig. 2f, the PFTS–SiO_2 coating without graphite powder has similar chemical elements as the coating with graphite. This indicates that the coating after spraying with aluminum phosphate contains a large number of elements in aluminum phosphate. However, the proportion of each element in the coating with graphite and without graphite varies slightly. Over here, the modifier used 1*H*,1*H*,2*H*,2*H*-perfluorooctanetrichlorosilane (PFTS), as it can take the shape of a micro-nano self-assembled monolayer structure on SiO_2 around without changing the microscopic shape of the coating surface. This is mainly because the modification of 1*H*,1*H*,2*H*,2*H*-perfluorooctyltrichlorosilane can not only reduce the surface free energy of the coating, but also increase the coating roughness to obtain superamphiphobicity. As shown in Fig. 2c and d, since the XRD peak intensity of the coating with graphite and without graphite is almost the same, their crystal form does not change significantly.

In addition, XPS was applied to measure the chemical elements and functional groups of PFTS–SiO_2 particles with graphite and without graphite. As shown in Fig. 3f, for the PFTS–SiO_2 particles without graphite, the XPS peaks observed at 103.5 eV, 134.5 eV, 284.8 eV and 533 eV were mainly assigned to

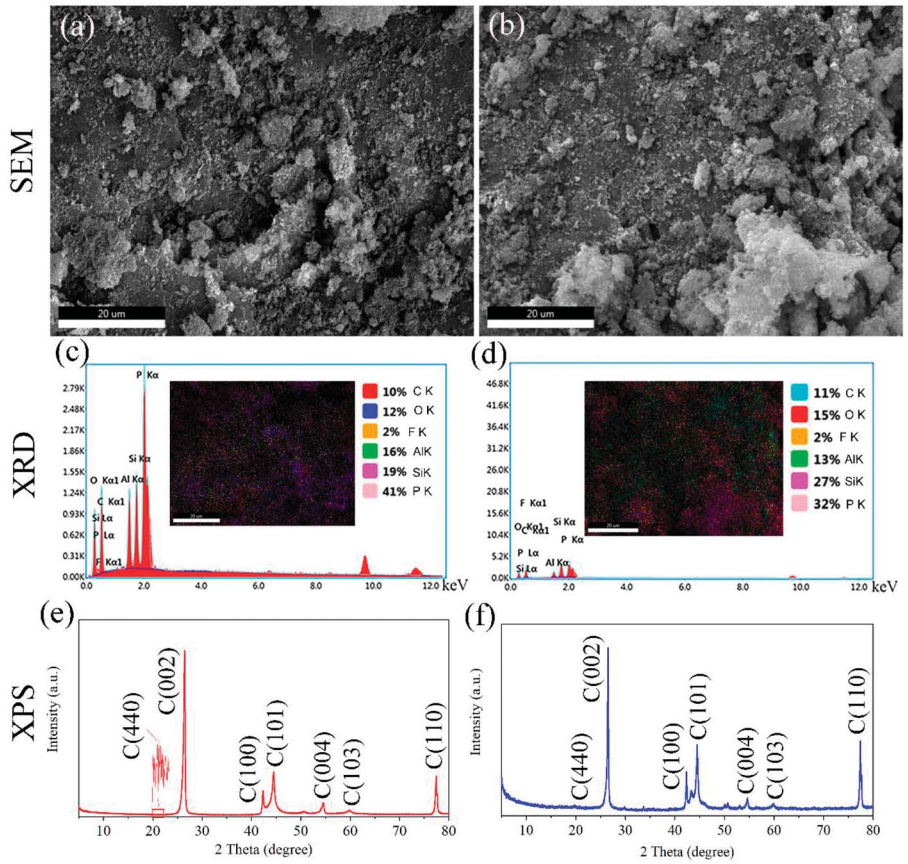

Fig. 2 Features of the prepared GPS coating. (a) SEM image, (c) EDS image, and (e) XRD spectrum of the PFTS–SiO_2 nanoparticles with graphite. (b) SEM image, (d) EDS image, and (f) XRD spectrum of the PFTS–SiO_2 nanoparticles without graphite.

Si, P, C and O. However, the XPS peak intensity of $-CF_2$ and $-CF_3$ of the PFTS–SiO_2 particles with graphite was slightly reduced (see Fig. 3d). The other peaks are basically the same as PFTS–SiO_2 particles with graphite. At the same time, the augment in the C peak intensity of PFTS–SiO_2 particles with graphite was mainly due to the introduction of graphite, which resulted in the presence of a good ideal of activated carbon atoms in the GPS coating. This activated carbon atom makes it easier for the $-CF_3$ groups in PFTS to modify SiO_2–graphite particles. It can be seen from the FT-IR spectrum of Fig. 4a that the absorption peaks of PFTS–SiO_2 particles without graphite appear at 3429.24 cm^{-1}, 1630.09 cm^{-1}, 1091.37 cm^{-1}, 950.71 cm^{-1} and 799.78 cm^{-1}, which were classified as $-NH_2$, –N═N–, $-C{=}CH_2$, –CHO and –C═CH– bending vibration, respectively. Similarly, the absorption peak intensity of the PFTS–SiO_2 particles with graphite is smaller than that of the PFTS–SiO_2 particles without graphite, but the absorption band of the absorption peak was the same as that of the PFTS–SiO_2 particles without graphite.

In addition, the thermogravimetry (TG) measurements were performed here at a dynamic heating rate of 10 °C min^{-1} in an air atmosphere to investigate the thermal stability of the prepared superamphiphobic GPS powder. In Fig. 4a, the main components of PFTS–SiO_2 without graphite are SiO_2 nanoparticles and 1*H*,1*H*,2*H*,2*H*-perfluorooctyltrichlorosilane (PFTS). The main components of PFTS–SiO_2 with graphite are SiO_2 nanoparticles, 1*H*,1*H*,2*H*,2*H*-perfluorooctyltrichlorosilane (PFTS) and graphite particles. It can be found from the thermogravimetric analysis curve that the thermolysis process is mainly within the range of 250–360 °C (see Fig. 4b), but the weight ratio the GPS power at the beginning of the decomposition is higher than the weight ratio without graphite. This indicates that adding graphite can improve the thermal stability of PFTS–SiO_2 particles. It is sufficient to satisfy the anti-greasy function of the carbon brush surface (the maximum temperature is 120–150 °C) of the hydroelectric generator system.

3.2. Serviceability of superamphiphobic GPS coating

Since the superamphiphobic GPS powder prepared is not very dependent on the substrate material, it can be coated on the surface of the carbon brush by spraying aluminum phosphate to form a superamphiphobic coating. This can not only realize the anti-greasy function of the carbon brush surface, but also realize the self-cleaning performance of the collector ring surface. *Via* observing the SEM image of the carbon brush surface with GPS coating (see Fig. 2b), it was found that the coated carbon brush surface presents a messy spherical protruding surface morphology. GPS powders got together to form a micron layered structure with a diameter in the range of 280–335 nm (see Fig. 6h), which is similar to the papillary protrusion structure on the surface of a lotus leaf.[16,24] At the same time, there are a large number of small particle clusters

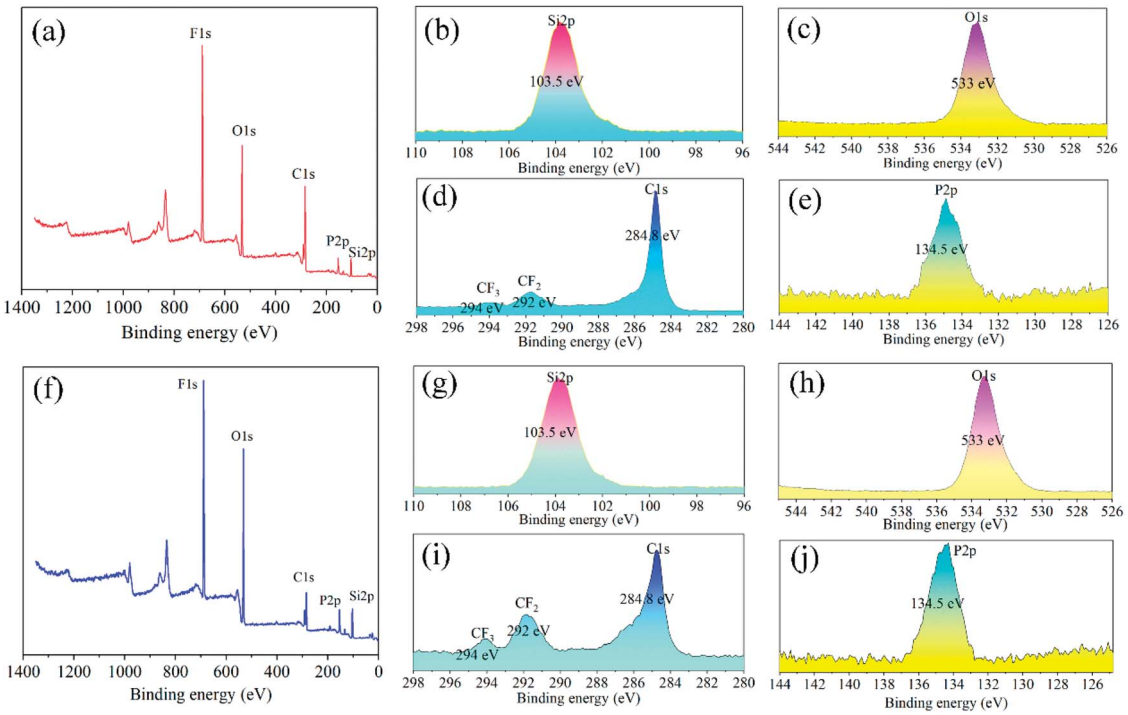

Fig. 3 XPS spectra of the superamphiphobic PFTS–SiO_2 nanoparticles. (a)–(e) XPS spectra of PFTS–SiO_2 nanoparticles with graphite. (f)–(j) XPS spectra of PFTS–SiO_2 nanoparticles without graphite.

around SiO_2, the diameter of which is tens of nanometers (see Fig. 6i). This is mainly due to the presence of graphite powder and the mixture with PFTS modifiers. In addition, the surface of the PFTS–SiO_2 particles is covered by small clusters with a diameter of about 10–20 nm (see Fig. 6h). Since the GPS particles have ideal oil and water surface contact angles (CAs $\geq$ 130°), the sliding angle is also low (SAs $\leq$ 9°) (see Fig. 5b and 9d), which indicates that the coating has excellent superamphiphobicity. It was also found that the surface of the uncoated carbon brush, glass and copper sheet all show significant hydrophilicity and lipophilicity, and oil and water completely wetted the substrate surface (see Fig. 6a–c).

In order to further investigate the effect of graphite content (10–20%, weight ratio with SiO_2) on the superoleophobicity of the GPS coating on the carbon brush surface, hexadecane was used as the test drop and the original carbon brush was used as the control sample. Here, when there is no coating on the carbon brush surface, the hexadecane drops onto the carbon brush surface and immediately wets the carbon brush surface (see Fig. 6c). The optical image in Fig. 6c displays the amphiphilicity of the uncoated carbon brush. As thought, as the graphite content increases (≤16%), the contact angles of the coated carbon brush decrease first and then increase and the contact angles are 134 ± 1.25°, 132.5 ± 1.5°, 133.5 ± 1.25°, 130 ± 1.5° and 136.5 ± 1.6°, respectively (Fig. 9c). However, as the graphite content continues to increase (>16%), the CA value on the coated carbon brush surface was greatly reduced to less than 130° (about 128.5°). This is mainly because graphite is

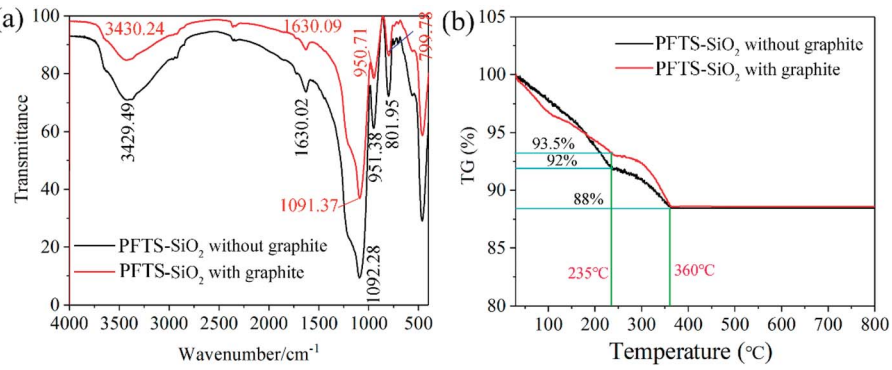

Fig. 4 (a) FT-IR spectra of PFTS–SiO_2 with and without graphite. (b) Thermogravimetric analysis curve of the as-prepared superamphiphobic powder with and without graphite.

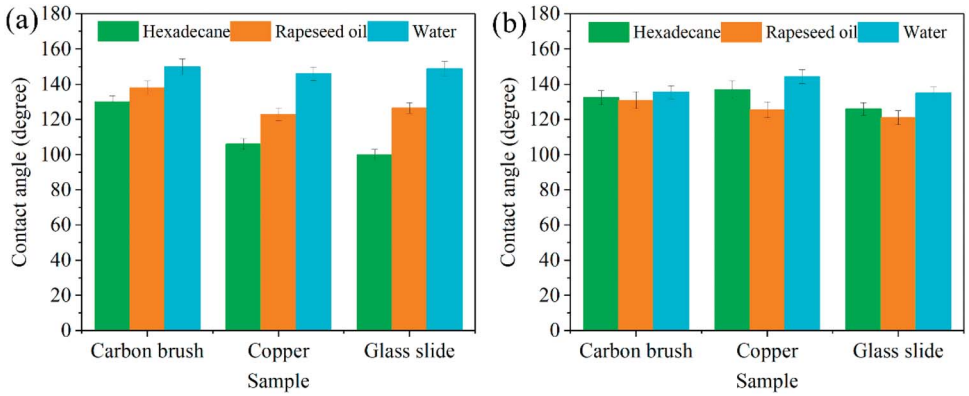

Fig. 5 Change curve of contact angle of different substrates. (a) CAs of the substrate surface without graphite. (b) Change in the contact angle of the superamphiphobic powder with graphite.

a lipophilic substance and when added in large quantities to the coating, it will reduce the superoleophobicity of the coating. To obtain the best conductivity and superoleophobicity of the coating, the content of graphite should be as small as possible while ensuring conductivity. Therefore, in this work, the graphite–PFTS–SiO_2 coating with a graphite content of 10% was selected for the relevant experiments. Fluorine is not only an electronegative element but also has a smaller size and a higher atomic polarizability.[35] Its atypical physical and chemical properties make it an exciting and valuable application in various fields, such as oil and water repellents.[36] Fluorine atoms with low polarizability lead to lower energy levels, which leads to lower molecular forces between fluorocarbon molecules. Low energy levels result in fluorocarbon-based tissues that are both oleophobic and hydrophobic. The $-CF_3-$ functional group is reported to have a very low surface free energy.[26] It can be seen from Fig. 10, the presence of the $-CF_3$ groups at the air interface of the carbon brush results in a decrease in the surface energy of these composite coatings (see Fig. 9d), resulting in the superamphiphobicity of the coated carbon brush surface.

In addition, hexadecane can roll from the coated carbon brush surface without wetting the surface of the carbon brush, and the SA is not more than 7° (see Fig. 9c). When the graphite content increased to 20%, the contact angle of the hexadecane droplet decreased to 128.5° and the sliding angle increased to 9°. It is precisely because of the increase in the graphite content that the lipophilic substances on the coating surface aggrandize, the surface CAs of the coated carbon brush decrease with the aggrandization of the graphite proportion in the superamphiphobic GPS coating, and the increase in the SAs is due to the increase in adhesion of the carbon brush surface. In addition, with the increase in graphite content, the number of $-CF_3$ groups in the coating significantly decreases, which weakens the superoleophobicity of the coated carbon brush surface, which further increases the possibility of the carbon brush surface being wetted by oily substances.

In addition to carbon brushes, superamphiphobic GPS particles can also be used to other surfaces of the material. Fig. 6 shows the wetting state and SEM images of uncoated glass plates, copper plates and carbon brushes and coated glass plates, copper plates and carbon brushes. Because of their amphiphilicity, water and organic solvents are completely wetted by the three original substrates (Fig. 6a–c). However, the three substrates of the coating can maintain the perfect spherical shape on the surface of liquids, such as water, rapeseed oil and hexadecane (Fig. 6d–f). In addition, the microstructure of the coated carbon brush substrate is also described. According to the aggregation of the superamphiphobic GPS powder on the surface of the coated carbon brush, micro-nano-level roughness was formed (Fig. 6g–i). The surface has a disordered nano-level irregular rough structure, which enables liquids such as water, rapeseed oil and hexadecane to maintain a nearly spherical shape on the surface of the carbon brush. To sum up, the combined effect of the micro-nano level structure on the coating surface and the inherent perfluoroalkyl group of PFTS reduces the surface energy of the contact surface, so that the prepared coating has excellent repellency to water and oil.

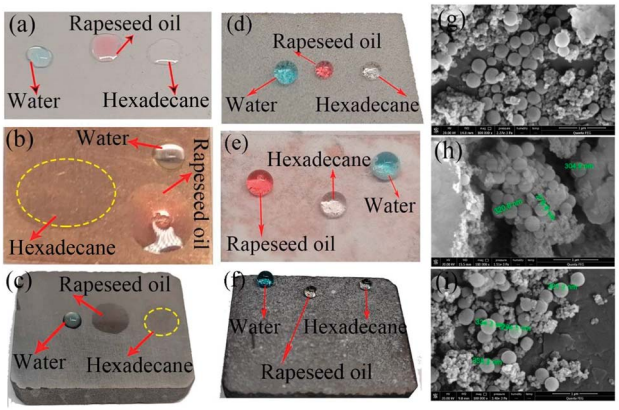

Fig. 6 Superamphiphobicity and surface morphology of different substrates coated with GPS. Wetting situation of water, hexadecane, and rapeseed oil droplets on the (a) uncoated glass sheet, (b) uncoated copper sheet, and (c) uncoated carbon brush. Wetting situation of water, hexadecane, and rapeseed oil droplets on the PFTS–SiO_2–graphite-coated (d) glass sheet, (e) copper sheet, and (f) carbon brush. (g–i) SEM images of GPS coated glass sheet, copper sheet and carbon brush.

3.3. Anti-greasy and self-cleaning performance of the coating

As a coating on the carbon brush surface, the carbon brush is always exposed to a harsh working environment filled with graphite powder, lubricating oil, dust and other pollutants.[37–39] The lubricating oil can wet the graphite powder and form a greasy substance. The greasy layer occupies microscopic pores on the coated surface and prevents the form of cavitation and solid–liquid composite interface, resulting in the loss of superamphiphobicity and the accumulation of pollutants. Therefore, the coating on the carbon brush surface must have self-cleaning and anti-oil adhesion performance to protect the coated surface from contamination. Here, we primarily tested the self-cleaning and anti-greasy properties of the superamphiphobic GPS coating on the carbon brush substrate, mainly because the greasy substance formed by graphite carbon powder and lubricating oil adheres to the carbon brush and collector ring. It is difficult to clean when greasy substances adhere to the surface of the collector ring and carbon brush; hence, graphite powder and rapeseed oil are used to test the self-cleaning and anti-greasy properties. It can be seen from Fig. 7a and b, when the droplets fall 2 cm above the carbon brush surface, the water droplets and rapeseed oil droplets can smoothly slide over the surface of the carbon brush and take away the graphite powder without causing the oil to wet the carbon powder and form greasy substances to pollute the carbon brush surface. Then, due to the high adhesion of the mixture of lubricating oil and graphite powder, serious pollution problems arise in the carbon brush/collector ring system of the hydroelectric generator. At the same time, few researchers have applied superamphiphobic coatings on carbon brushes to make them have reliable anti-greasy properties. Therefore, after soaking the carbon brush coated with a superamphiphobic coating in the polluted solution of rapeseed oil and graphite powder for 30 min, it still has a clean surface and no residual greasy substances, showing excellent anti-greasy properties.

In addition, on behalf of studying the anti-greasy properties of the collector ring, the anti-greasy performance of 304 stainless steel coated with GPS coating was also trialed. To highlight the anti-greasy performance of the coating, a comparative experiment of uncoated stainless steel was carried out. When the uncoated and coated stainless steel substrates were immersed in a mixture of graphite powder and rapeseed oil, respectively, a number of greasy substances adhered to the surface of the uncoated stainless steel. However, the coated stainless steel surface remained clean (see Fig. 8). The results show that the prepared superamphiphobic GPS coating has excellent anti-greasy properties on the carbon brush and collector ring. This is mainly to form air pockets between the micro-nanostructures of the coating and the liquid to keep off contaminants from adhering to the surface of the coating. In particular, the anti-greasy properties in the mixed solution of rapeseed oil and graphite show that the superamphiphobic GPS coating has excellent anti-greasy properties for carbon brushes and collector rings. In summary, the self-cleaning and anti-greasy properties of the superhydrophobic GPS coating will endow them with broad application prospects including hydropower, wind power, and transportation.

3.4. Mechanical properties and conductivity of the coating

Here, the mechanical properties of the superamphiphobic GPS coating on the surface of the carbon brush were first evaluated by pressing with bare hands and fingers.[40] If the surface of the above coating is very fragile, the force applied on the contact area will alter the micromorphology of the coating and damage the contact part or even make the coating lose its hydrophobic and oleophobic properties. In addition, pressing the surface

Fig. 7 Anti-greasy and self-cleaning performance of coated carbon brushes. (a) Water and (b) rapeseed oil can rapidly roll off and take away the graphite powder on the tilted coating carbon brush. (c) Antifouling effect of coated and uncoated carbon brushes in water. (d) Antifouling effect of coated and uncoated carbon brushes in rapeseed oil.

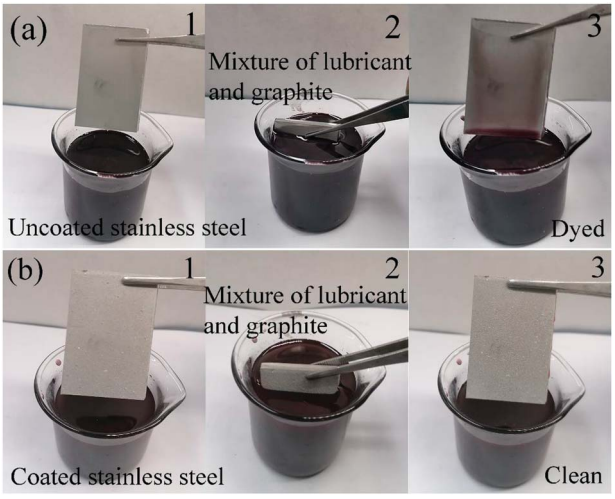

Fig. 8 Self-cleaning and anti-greasy performance of stainless steel: (a) uncoated stainless steel and (b) coated stainless steel.

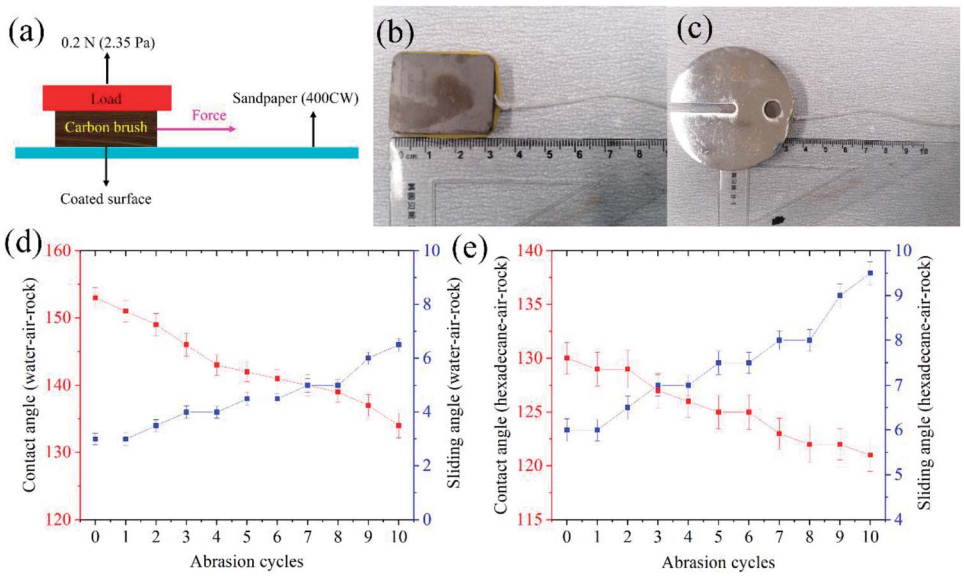

Fig. 9 (a) Schematic diagram used to assess the mechanical wear resistance of a GPS coating. Physical images used to assess the mechanical wear resistance of GPS coatings: (b) no normal pressure and (c) normal pressure. CAs and SAs of water and hexadecane on the coated carbon brush surface change with the abrasion cycle: (d) water and (e) hexadecane.

with fingers will cause salt and oil pollution, which will reduce the surface roughness of the superamphiphobic coating microstructure. It was found that after pressing with a finger, the superamphiphobic performance of the carbon brush coated with superamphiphobic GPS remained unchanged.

In the next moment, so as to study the mechanical wear resistance of the superamphiphobic GPS coating, a simple wear test was carried out.[40,41] In this wear experiment, under 0.2 N normal force (pressure 2.35 Pa), a 400CW sandpaper with a length of 30 cm was used as the abrasion surface, and the surface of the carbon brush coated with a superamphiphobic

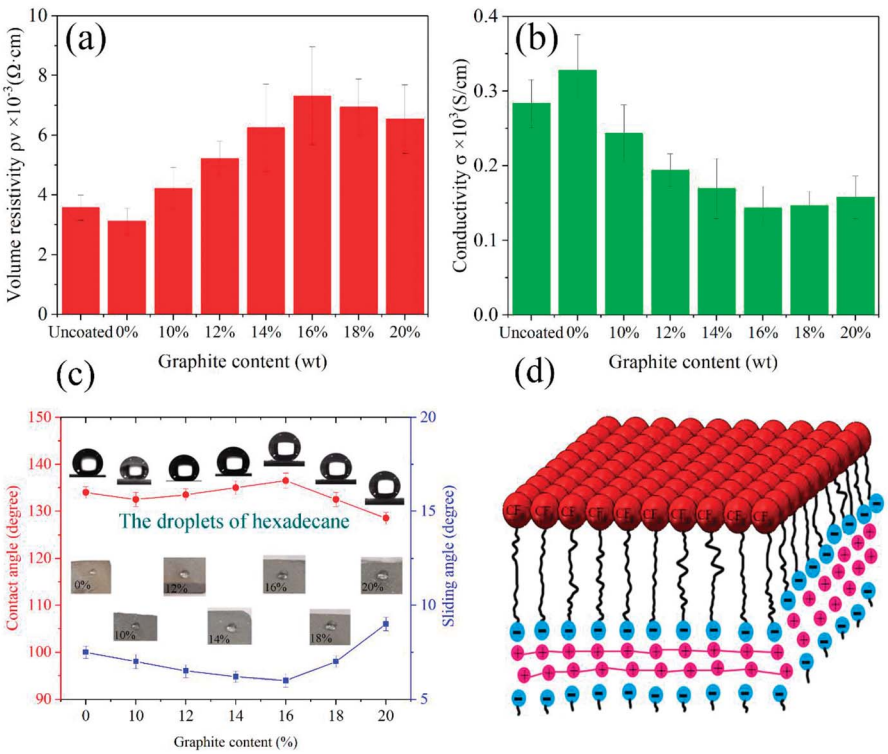

Fig. 10 Conductivity of coated carbon brushes. (a) Diagram of volume resistivity change with graphite content. (b) Graph of the change in conductivity with graphite content. (c) Contact angle changes with the graphite content. (d) Mechanism diagram of graphite–SiO_2 particles modified by PFTS.

coating moves unidirectionally on the surface of the sandpaper (Fig. 9a). Fig. 9b and c show the actual picture of carbon brush abrasion with and without load. Fig. 10d and e show that the change in the CAs and SAs of water and hexadecane dropped on the surface of the carbon brush coated with superamphiphobic GPS with the abrasion cycle. It can be seen from Fig. 9 that after 10 cycles of wear, the hydrophobicity of the GPS coating is still very excellent, but its superoleophobicity decreases after about 8 cycles.

The excellent abrasion resistance of the superamphiphobic GPS coating of the carbon brush is mainly put down to the prefabricated stratified structure that captures the abrasive dust in the micro-nano structure of the coating surface. In addition, the large amount of air captured in multi-scale terrain can reduce the frictional damage. The self-lubricating properties of SiO_2 macromolecules and embedded graphite also help the coating to withstand long-term abrasion without significantly reducing the superamphiphobicity. This abrasion-resistant coating must essentially be kept clean in the non-wearing surface of the carbon brush/collector ring in the excitation system of the hydroelectric generator:

The conductivity of the coating can be theoretically derived from eqn (3) as follows:[37,42–44]

$$\sigma = \frac{l}{RA} = \frac{l}{R(wh)} = \frac{l}{w}\frac{1}{Rh} \quad (3)$$

where σ is the conductivity [S m^{-1}], l is the length of the GPS coating between electrodes [m], A is the cross-sectional area of the coating [m^2], and R is the coating resistance [Ω].[45] To study the conductivity of the GPS coating experimentally, the surface resistivity of the GPS coating was measured using a four-probe surface resistivity meter (Laiesta-GP Model MCP-T610). An electrochemical workstation (Produced by Shanghai Chenhua Instrument Co., Ltd.) was used to measure the changes in the current and impedance of the carbon brush with and without coating over time. During the test, the negative pole of the circuit was fixed, and the positive pole slid on the surface of the carbon brush to measure the current and impedance changes on the carbon brush surface during the sliding process.

It can be seen from Fig. 10a that the conductivity of the carbon brush coating by and by increases with the increase in graphite content, indicating that addition of graphite can enhance the conductivity of the coating. As shown in Fig. 10b, the volume resistivity of the carbon brush coating decreases with the increase in graphite content, indicating that the increase in graphite content reduces the resistance of the coating. From the two above-mentioned aspects, the addition of graphite can improve the conductivity of the coating. Unfortunately, however, the liquid repellency of the coating becomes worse and worse with the increase in graphite content (see Fig. 10c). This is mainly because graphite is a flat material that reduces the surface roughness, so that the rough structure of the coating surface is filled with graphite and becomes no longer rough. At the same time, the cavitation effect in the rough structure is inhibited, resulting in a smaller contact angle on the coating surface. In addition, graphite's unique covalent

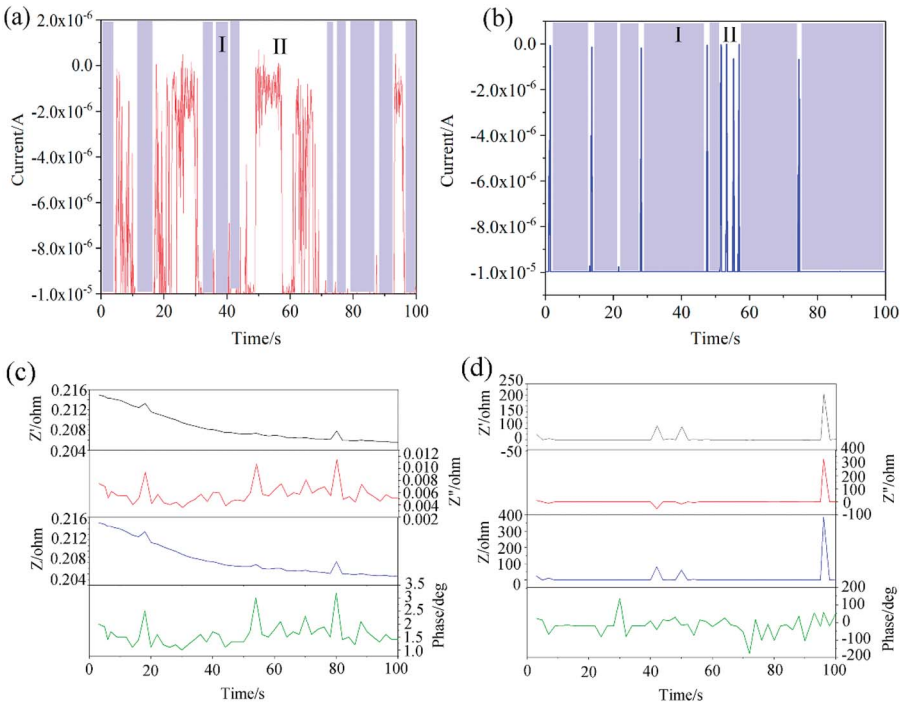

Fig. 11 Characteristic curve of the current of the coated and uncoated carbon brush over time. (a) Curve of the current of the coated carbon brush over time. (b) Curve of the current of the uncoated carbon brush over time. The characteristic curve of the impedance of the coated and uncoated carbon brush over time. (c) Curve of the impedance of the coated carbon brush over time. (d) Curve of the impedance of the uncoated carbon brush over time.

molecules and emitted electrons make it an excellent conductor of electricity. When current passes through the GPS coating, these freely moving electrons and the $-CF_3$ group in the Perfluorooctyltrichlorosilane form the interaction between electrons (see Fig. 10d). This is one of the reasons that adding graphite to the coating can improve the conductivity of the coating.

As shown in Fig. 11a and b, the region with the minimum and stable value of current change over time is called I, and the region with a large range of current fluctuation is called II. It can be seen from Fig. 11 that the area of region I where the surface current of the coated carbon brush changes is smaller than the area of region I of the uncoated carbon brush. Region II of the coated carbon brush is larger than region II of the uncoated carbon brush. This indicates that although the coating can conduct electricity, the stability of conduction is worse than that of the uncoated surface. In addition, Fig. 11c and d show the impedance over time for both coated and uncoated carbon brushes. In Fig. 11c and d, Z' expresses the real part of the impedance, Z'' expresses the imaginary part of the impedance, and Z represents the modulus of the impedance. As shown in Fig. 11, the impedance value range of the coated carbon brush surface is small and shows a gradually decreasing trend. However, the impedance value of the uncoated carbon brush surface has just begun to level off, and then a sharp peak appears. This indicates that the surface resistance of the uncoated carbon brush will have a steep increase in resistance over time. This is also one of the reasons that the carbon brush sparks under actual working conditions. The coating is one of the measures to solve the carbon brush sparking during actual operation.

4. Conclusions

In summary, a SiO_2 powder has been prepared *via* a reduction reaction, and modified with 1*H*,1*H*,2*H*,2*H*-perfluorooctyltrichlorosilane to form the PFTS–SiO_2 powder, and graphite has been mixed into the above powder in a certain proportion to obtain the superamphiphobic graphite–PFTS–SiO_2 powder. Due to its weak dependence on the substrate, it can put into use all kinds of material surfaces such as carbon brushes, glass sheets, copper sheets, and stainless steel and can also be applied to prepare multifunctional conductive superamphiphobic sprayed coatings. The prepared coating has liquid repellency to water, hexadecane, rapeseed oil and other solutions. In addition, the self-cleaning, anti-greasy, mechanical and conductive functions reported in this paper have broad application potentiality in engineering applications such as surface engineering and environmental engineering. The greatest advantage of the coating is that it has anti-adhesion to the mixed solution of rapeseed oil and graphite powder, so that the mixed solution has no residual flow on the coating surface. More importantly, the coating has excellent conductivity, so it can be applied to the carbon brush/collector ring conductive system of hydropower. Finally, due to its excellent electrical conductivity, the coating is of great significance in engineering fields such as current carrying friction and current conduction.

Conflicts of interest

There are no conflicts to declare.

Acknowledgements

This work is supported by the National Nature Science Foundation of China (No 51735013), the Tribology Science Fund of State Key Laboratory of Tribology (SKLTKF19B09), the open fund project of the State Key Laboratory of Solid Lubrication, Lanzhou Institute of Chemical Physics, Chinese Academy of Sciences (LSL-1909).

References

1 X.-Z. Lin, M.-H. Zhu, J.-L. Mo, G.-X. Chen, X.-S. Jin and Z.-R. Zhou, *Trans. Nonferrous Met. Soc. China*, 2011, **21**, 292–299.
2 D.-K. Lawson and T.-A. Dow, *Wear*, 1985, **102**, 105–125.
3 D.-Z. Wang, C.-F. Yu, J. Ma, W. Liu and Z.-J. Shen, *Mater. Sci. Technol.*, 2017, **34**, 172–178.
4 J.-T. Xia, Z.-L. Hu, Z.-H. Chen and G.-Y. Ding, *Trans. Nonferrous Met. Soc. China*, 2007, **17**, 1379–1384.
5 E.-I. Shobert, *Trans. Am. Inst. Electr. Eng., Part 3*, 1954, **73**, 788–799.
6 Q.-Z. Teng, X. Tan, Z.-Y. Wu, J. Shen and H.-F. Wang, *Acta Phys. Sin.*, 2015, **64**, 421–427.
7 K.-H. Cho, U.-S. Hong, K.-S. Lee and H. Jang, *Tribol. Lett.*, 2007, **27**, 301–306.
8 H.-J. Yang, G.-X. Chen, S.-D. Zhang and W.-H. Zhang, *Proc. Inst. Mech. Eng., Part J*, 2012, **226**, 722–728.
9 T. Ding, G.-X. Chen, J. Bu and W.-H. Zhang, *Wear*, 2011, **271**, 1629–1636.
10 I. Yasar, A. Canakci and F. Arslan, *Tribol. Int.*, 2007, **40**, 1381–1386.
11 N. Argibay, J.-A. Bares, J.-H. Keith, G.-R. Bourne and W.-G. Sawyer, *Wear*, 2010, **268**, 1230–1236.
12 G. Toth, J. Mäklin, N. Halonen, J. Palosaari, J. Juuti, H. Jantunen, K. Kordas, W. G. Sawyer, R. Vajtai and P. M. Ajayan, *Adv. Mater.*, 2009, **21**, 2054–2058.
13 Y. Wu, M. Y. Zhao and Z. G. Guo, *Chem. Eng. J.*, 2018, **334**, 1584–1593.
14 H. Zhou, H. Wang, H. Niu, A. Gestos and T. Lin, *Adv. Funct. Mater.*, 2013, **23**, 1664–1670.
15 X. Deng, L. Mammen, H.-J. Butt and D. Vollmer, *Science*, 2012, **335**, 67–70.
16 L. W. Chen, Z. G. Guo and W. M. Liu, *ACS Appl. Mater. Interfaces*, 2016, **8**, 27188–27198.
17 X. Xue, C. Yu, J. Wang and L. Jiang, *ACS Nano*, 2016, **10**, 10887–10893.
18 Y. M. Zheng, X. F. Gao and L. Jiang, *Soft Matter*, 2007, **3**, 178–182.
19 W. W. Xu, Z. Y. Lu, X. M. Sun, L. Jiang and X. Duan, *Acc. Chem. Res.*, 2018, **51**, 1590–1598.
20 L. C. Peng, Y. H. Meng and H. Li, *Cellulose*, 2016, **23**, 2073–2085.

21 C. Zhang, B. Zhang, H. Ma, Z. Li, X. Xiao, Y. Zhang, X. Cui, C. Yu, M. Cao and L. Jiang, *ACS Nano*, 2018, **12**, 2048–2055.
22 X. Xiao, C. Zhang, H. Ma, Y. Zhang, G. Liu, M. Cao, C. Yu and L. Jiang, *ACS Nano*, 2019, **13**, 4083–4090.
23 Y. J. Yin, R. H. Huang, W. Zhang, M. Zhang and C. X. Wang, *Chem. Eng. J.*, 2016, **289**, 99–105.
24 Z. G. Guo, W. M. Liu and B.-L. Su, *J. Colloid Interface Sci.*, 2011, **353**, 335–355.
25 H. Bellanger, T. Darmanin, E. T. de Givenchy and F. Guittard, *Chem. Rev.*, 2014, **114**, 2694–2716.
26 T. Nishino, M. Meguro, K. Nakamae, M. Matsushita and Y. Ueda, *Langmuir*, 1999, **15**, 4321–4323.
27 C. Söz, E. Yilgör and I. Yilgör, *Polymer*, 2016, **99**, 580–593.
28 F. Xiao, S. J. Yuan, B. Liang, G. Q. Li, S. O. Pehkonen and T. J. Zhang, *J. Mater. Chem. A*, 2015, **3**, 4374–4388.
29 Y. F. Si, Z. G. Guo and W. M. Liu, *ACS Appl. Mater. Interfaces*, 2016, **8**, 16511–16520.
30 C. Lee and C. J. Kim, *Phys. Rev. Lett.*, 2011, **106**, 014502.
31 C. K. Söz, E. Yilgör and I. Yilgör, *Prog. Org. Coat.*, 2015, **84**, 143–152.
32 S. Amini, S. Kolle, L. Petrone, O. Ahanotu, S. Sunny, C. N. Sutanto, S. Hoon, L. Cohen, J. C. Weaver, J. Aizenberg, N. Vogel and A. Miserez, *Science*, 2017, **357**, 668–673.
33 E. Yilgör and I. Yilgör, *Prog. Polym. Sci.*, 2014, **39**, 1165–1195.
34 Z. K. He, M. Ma, X. R. Lan, F. Chen, K. Wang, H. Deng, Q. Zhang and Q. Fu, *Soft Matter*, 2011, **7**, 6435–6443.
35 A. Bondi, *J. Phys. Chem.*, 1964, **68**, 441–451.
36 P. Meng, S. Deng, Z. Du, B. Wang and B. Xing, *Sci. Rep.*, 2017, **7**, 44694.
37 T. Cheng, H. Ren, Q. Zhang, X. Zhan and F. Chen, *J. Mater. Chem. A*, 2015, **3**, 21637–21646.
38 W. Peng, X. Gou, H. Qin, M. Zhao, X. Zhao and Z. Guo, *Chem. Eng. J.*, 2018, **352**, 774–781.
39 N. Li, W. Chen, G. Chen, X. Wan and J. Tian, *ACS Sustainable Chem. Eng.*, 2018, **6**, 6370–6377.
40 J. Ma, X. Y. Zhang, D. P. Wang, D. Q. Zhao, D. W. Ding, K. Liu and W. H. Wang, *Appl. Phys. Lett.*, 2014, **104**, 173701.
41 M.-K. Tang, X.-J. Huang, X.-W. Li, Z.-Y. Huang, S.-M. Zhang and Q.-X. Zhang, *Mater. Express*, 2016, **6**, 101–115.
42 Z. Zhao, H. Chen, X. Liu, H. Liu and D. Zhang, *Surf. Coat. Technol.*, 2018, **349**, 340–346.
43 M.-Y. Li, M. Yang, E. Vargas, K. Neff, A. Vanli and R. Liang, *Meas. Sci. Technol.*, 2016, **27**, 095004.
44 L. Jayasinghe, Y. Gu and N. Narendran, *Proc. SPIE-Int. Soc. Opt. Eng.*, 2006, **149**, 20.
45 A. Baldelli, J. Ou, D. Barona, W. Li and A. Amirfazli, *Adv. Mater. Interfaces*, 2020, **8**, 1902110.